AD NUMBER

AD003750

NEW LIMITATION CHANGE

TO

Approved for public release, distribution unlimited

FROM

Distribution authorized to U.S. Gov't. agencies and their contractors; Administrative/Operational Use; FEB 1953. Other requests shall be referred to Office of Naval Research, 800 North Quincy Street, Arlington, VA 22217-5660.

AUTHORITY

ONR ltr., 9 Nov 1977

AD-

3750

Columbia University
in the City of New York

DEPARTMENT OF CIVIL ENGINEERING

REFLECTION OF FLEXURAL WAVES AT THE EDGE OF A PLATE

By

T. R. KANE

Office of Naval Research Project NR-064-388
Contract Nonr-266(09)
Technical Report No. 6
CU-7-53-ONR-266(09)-CE
February 1953

ABSTRACT

The reflection of straight-crested flexural waves at the edge of a semi-infinite plate is studied in terms of a two-dimensional plate theory. It is found that, in general, a flexural wave propagated toward the edge at an arbitrary angle of incidence gives rise to three reflected waves: two flexural waves and a shear wave. A number of special cases, involving degenerate forms of these motions, are investigated in detail.

1. Introduction

In this paper Mindlin's [1][1] equations of flexural motions of plates are used to study the reflection of a straight-crested wave at the edge of a semi-infinite plate. The equations accommodate three modes of motion: two types of flexural waves and a thickness-shear wave. It is found that, in general, all three of these motions are excited upon incidence of any one of them at a free edge. The shear motion, here encountered, is of particular interest; for this motion is absent in the classical theory of plates, whence the applicability of that theory is restricted to a range of frequencies considerably below that corresponding to the first mode of thickness-shear vibration. By the same token, the present theory does not include the higher modes of motion which are to be found in three-dimensional elasticity theory; thus, the solution set forth below may be expected to furnish an adequate description for frequencies which do not materially exceed that of the first thickness-shear mode.

The character of the reflected waves is affected by both the angle of incidence and the ratio of plate thickness to wave-length of the incident wave. Appropriate values of these two parameters give rise to such special cases as waves whose amplitudes decrease exponentially with distance from the edge, vibrations, resonance, disappearance of some of the reflected waves, and, for grazing incidence, complete disappearance of the motion.

Following a resumé of the plate equations in Section 2, straight-crested waves are considered in Section 3. Incident and emergent waves are described in Section 4 and, in terms of these, a formal solution is reached in Section 5. In Sections 6 and 7 various cases of normal and oblique incidence are discussed in detail. Section 8 deals with grazing incidence.

1. Numbers in brackets refer to the Bibliography at the end of the paper.

2. Plate Displacements, Equations of Motion and Stresses

For a plate of thickness h, oriented as in Fig. 1, plate displacements $\psi_x(x,y,t)$, $\psi_y(x,y,t)$ and $w(x,y,t)$ are given by (see [1])

$$\begin{aligned} \psi_x &= \left[(\sigma_1-1)\frac{\partial w_1}{\partial x} + (\sigma_2-1)\frac{\partial w_2}{\partial x} + \frac{\partial H}{\partial y}\right]e^{ipt} \\ \psi_y &= \left[(\sigma_1-1)\frac{\partial w_1}{\partial y} + (\sigma_2-1)\frac{\partial w_2}{\partial y} - \frac{\partial H}{\partial x}\right]e^{ipt} \\ w &= (w_1+w_2)e^{ipt} \end{aligned} \tag{1}$$

The functions $w_1(x,y)$, $w_2(x,y)$ and $H(x,y)$ are governed, respectively, by equations of motion

$$\begin{aligned} (\nabla^2+\delta_1^2)w_1 &= 0 \\ (\nabla^2+\delta_2^2)w_2 &= 0 \\ (\nabla^2+\omega^2)H &= 0 \end{aligned} \tag{2}$$

In the above,

$$(\sigma_1, \sigma_2) = (\delta_2^2, \delta_1^2)(R\delta_0^4 - S^{-1})^{-1} = (\delta_1^{-2}, \delta_2^{-2})S\delta_0^4$$

$$2(\delta_1^2, \delta_2^2) = \delta_0^4\{S+R \pm [(S-R)^2+4\delta_0^{-4}]^{1/2}\} \tag{3}$$

$$(1-\nu)\omega^2 = 2(R\delta_0^4 - S^{-1}) \tag{4}$$

$$D\delta_0^4 = \rho p^2 h \tag{5}$$

$$R = \frac{h^2}{12}, \quad S = \frac{D}{\kappa^2 \mu h}$$

$$D = \frac{Eh^3}{12(1-\nu^2)}, \tag{6}$$

p is the circular frequency associated with the wave motion. E, ν, ρ are, respectively, Young's Modulus, Poisson's Ratio, and the mass density of the plate material.

Plate bending moments M_x, M_y, shears Q_x, Q_y and twisting moment M_{yx} are given by

$$
\begin{aligned}
M_x &= D\left(\frac{\partial \Psi_x}{\partial x} + \nu \frac{\partial \Psi_y}{\partial y}\right) \\
M_y &= D\left(\frac{\partial \Psi_y}{\partial y} + \nu \frac{\partial \Psi_x}{\partial x}\right) \\
2M_{yx} &= D(1-\nu)\left(\frac{\partial \Psi_y}{\partial x} + \frac{\partial \Psi_x}{\partial y}\right) \\
Q_x &= \kappa^2 \mu h \left(\Psi_x + \frac{\partial w}{\partial x}\right) \\
Q_y &= \kappa^2 \mu h \left(\Psi_y + \frac{\partial w}{\partial y}\right)
\end{aligned}
\quad , \tag{7}
$$

μ is the modulus of rigidity of the plate material. The definition of κ^2 is given in [1].

3. Straight-Crested Waves

Taking any one of the functions w_1, w_2, or H to be of the form

$$A \exp(i\xi x), \quad \xi > 0$$

and letting the remaining two vanish identically, we find that, in each case, two of the equations of motion are automatically satisfied while the remaining

one requires that

$$\gamma^2 = \begin{cases} \delta_1^2\,; & W_1 \neq 0,\quad W_2 = H = 0 \\ \delta_2^2\,; & W_2 \neq 0,\quad W_1 = H = 0 \\ \omega^2\,; & H \neq 0,\quad W_1 = W_2 = 0 \end{cases} \tag{8}$$

Letting

$$p^2 = (\gamma c)^2, \quad c > 0,$$

this leads to [see Equations (3), (4), (5)] three possible types of relationships between phase velocity C and wave number γ :

$$\frac{c}{c_s} = \begin{cases} \dfrac{K}{\gamma}\left[\dfrac{\Gamma - (\Gamma^2 - 4\gamma^2 RS)^{1/2}}{2K}\right]^{1/2}; & W_1 \neq 0,\quad W_2 = H = 0 \\ \dfrac{K}{\gamma}\left[\dfrac{\Gamma + (\Gamma^2 - 4\gamma^2 RS)^{1/2}}{2R}\right]^{1/2}; & W_2 \neq 0,\quad W_1 = H = 0 \\ \dfrac{K}{\gamma}\left[\dfrac{2 + \gamma^2(1-\nu)S}{R}\right]^{1/2}; & H \neq 0,\quad W_1 = W_2 = 0 \end{cases} \tag{9}$$

where

$$\Gamma = 1 + \gamma^2(R+S)$$

and C_s is the velocity of shear waves in an infinite medium. A plot of c/c_s versus $h\gamma$ (with $\nu = 1/4$) for each of these cases is shown in Fig. 3. It is seen that $c/c_s \to 0$ as $h\gamma \to 0$ for a W_1 wave, while $c/c_s \to \infty$ as $h\gamma \to 0$ for W_2 and H waves. In the sequel we shall call W_1 a "slow" flexural wave, W_2 a "fast" flexural wave and H a shear wave. (The fact that the preceding discussion involves waves propagated in the X -direction, does not result in any loss of generality.)

4. Incident and Emergent Waves

Referring the semi-infinite plate to axes x, y, z as shown in Fig. 2 we consider a slow flexural wave[2] propagated towards the edge of the plate,

$$w_1 = Ae^{i\gamma\psi}, \quad w_2 = H = 0 \tag{10}$$

where

$$\psi = y\sin\alpha - x\cos\alpha$$

We postulate three emergent waves, propagated respectively towards P', P'', P''' as shown in Fig. 2. These are

a) a slow flexural wave:

$$w_1' = A'e^{i\gamma'\psi'}, \quad w_2' = H' = 0 \tag{11}$$

b) a fast flexural wave:

$$w_2'' = A''e^{i\gamma''\psi''}, \quad w_1'' = H'' = 0 \tag{12}$$

c) a shear wave:

$$H''' = A'''e^{i\gamma'''\psi'''}, \quad w_1''' = w_2''' = 0 \tag{13}$$

where

$$\psi^j = y\sin\alpha^j + x\cos\alpha^j, \quad j = {}', {}'', {}'''$$

and the α^j are the angles of emergence shown in Fig. 2.

In accordance with Equations (9), these waves are propagated with velocities c^j which depend on their respective wave numbers γ^j.

2. The case of a fast incident wave is similar in nature and will not be discussed in the present paper.

The displacements corresponding to these waves are obtained from Equation (1). Denoting the incident wave by w, ψ_x and ψ_y, and calling the displacement components of the emergent waves w^j, ψ_x^j, ψ_y^j $(j = {}', {}'', {}''')$, we observe that, since the equations of motion (2) are linear, the state of motion given by

$$
\begin{aligned}
w^* &= w + \sum_j w^j \\
\psi_x^* &= \psi_x + \sum_j \psi_x^j \\
\psi_y^* &= \psi_y + \sum_j \psi_y^j
\end{aligned}
\tag{14}
$$

is a possible state of motion for an infinite plate. For the semi-infinite plate under consideration, three boundary conditions must be satisfied on the edge $x = 0$.

5. Boundary Conditions

Plate stresses M_x^*, M_y^*, etc. corresponding to the motion defined by Equations (14) may be computed from Equations (7). To obtain a traction-free edge, we must have, on $x = 0$,

$$M_x^* = M_{yx}^* = Q_y^* = 0 . \tag{15}$$

In order that these equations be satisfied for all values of the time t and all values of the space variable y, it is necessary that the circular frequencies p and p^j associated with the various waves be identical, i.e.,

$$fc = f^j c^j , \tag{16}$$

and that the angles α and α^j satisfy

$$f \sin\alpha = f^j \sin\alpha^j . \tag{17}$$

Now, the relation between C and f is of the same form as that between C' and f', both being slow flexural waves. Thus it follows from Equations (16) and (17) that the angle of emergence α' of the slow flexural wave is equal to the angle of incidence α of the incident wave, and that the wave numbers and phase velocities of these two waves are identical. Equations (16) and (17) show, furthermore, that the condition of vanishing traction at the edge of the plate, [Eq. (15)], leads to a determination of the phase velocity, wave number and angle of emergence of each of the postulated emergent waves when the angle of incidence and wave number (or phase velocity) of the incident wave are specified.

The boundary conditions (15) also impose restrictions on the amplitude ratios A^j/A. From Equations (10)-(13), (14) and (7) we get, upon substitution into Equations (15), a system of three non-homogeneous linear algebraic equations governing these amplitude ratios,

$$\sum_j \phi_n^j \frac{A^j}{A} = -\frac{2}{\sqrt{2}}\, \phi_n' \cos\left[(2n-1)\frac{\pi}{4}\right], \quad j = {}', {}'', {}''' ; \quad n = 1,2,3 \tag{18}$$

where

$$\begin{aligned}
\phi_1^j &= M^j Q^j, \quad j = {}', {}'' \\
\phi_1''' &= (1-\nu) f'''^2 \sin\alpha''' \cos\alpha''' \\
\phi_2^j &= M^j \sin 2\alpha^j, \quad j = {}', {}'' \\
\phi_2''' &= -f'''^2 \cos 2\alpha''' \\
\phi_3^j &= S\delta_0^4 f (f^j)^{-1} \cos\alpha^j, \quad j = {}', {}'' \\
\phi_3''' &= f^2 \sin\alpha
\end{aligned} \tag{19}$$

with

$$M^j = S\delta_0^4 - (\gamma^j)^2$$

$$\theta^j = \cos^2\alpha^j + \nu \sin^2\alpha^j .$$

The analog, in the present theory, to F. Neumann's uniqueness theorem [2] guarantees that the above constitutes the unique solution of the problem. We may say then that a slow incident flexural wave produces, in general, three reflected waves: a slow flexural, a fast flexural, and a shear wave.

6. Normal Incidence

We now proceed to study the character of the reflected waves in terms of the angle of incidence α and the wave number γ of the incident wave. We begin by examining the case of normal incidence, i.e., $\alpha = 0$.

The wave numbers γ'' and γ''' of the fast reflected wave and of the shear wave are given by [see Eqs. (8), (4), (5)]

$$2(\gamma'')^2 = \delta_0^{-4}\{S+R-[(S-R)^2+4\delta_0^{-4}]^{1/2}\} \tag{20}$$

$$(\gamma''')^2 = 2(1-\nu)^{-1}(R\delta_0^4 - S^{-1}) \tag{21}$$

Both γ'' and γ''' vanish when $RS\delta_0^4 = 1$, i.e., when $\gamma^2 RS = R+S$. For $\gamma^2 RS < R+S$, γ'' and γ''' are imaginary while for $\gamma^2 RS > R+S$ both are real. The physical significance of $\gamma^2 RS = 1$ will be discussed when the motion corresponding to that value of the wave number of the incident wave has been determined. We first consider

$$\underline{\gamma^2 RS < R+S}$$

From Eq. (17) we have, for $\alpha = 0$,

$$\alpha^j = 0, \quad j = ', '', '''$$

The amplitude ratios are found from Eqs. (18):

$$\begin{aligned}
\frac{A'}{A} &= \frac{a_1}{A} + i\frac{b_1}{A} \\
\frac{A''}{A} &= \frac{a_2}{A} + i\frac{b_2}{A} \qquad\qquad (22) \\
\frac{A'''}{A} &= 0
\end{aligned}$$

where

$$\frac{a_1}{A} = \frac{(\xi'')^2(S\delta_0^4+\xi''^2)^2 - \gamma^2(S\delta_0^4-\gamma^2)^2}{(\xi'')^2(S\delta_0^4+\xi''^2)^2 + \gamma^2(S\delta_0^4-\gamma^2)^2}$$

$$\frac{b_1}{A} = -\frac{2\xi''\gamma(S\delta_0^4+\xi''^2)(S\delta_0^4-\gamma^2)}{(\xi'')^2(S\delta_0^4+\xi''^2)^2+\gamma^2(S\delta_0^4-\gamma^2)^2}$$

$$\frac{a_2}{A} = -\frac{2\xi''^2(S\delta_0^4+\xi''^2)(S\delta_0^4-\gamma^2)}{\xi''^2(S\delta_0^4+\xi''^2)^2+\gamma^2(S\delta_0^4-\gamma^2)^2}$$

$$\frac{b_2}{A} = \frac{2\xi''\gamma(S\delta_0^4-\gamma^2)^2}{\xi''^2(S\delta_0^4+\xi''^2)^2+\gamma^2(S\delta_0^4-\gamma^2)^2}$$

and

$$\bar{\xi}'' = -i\gamma',$$

so that ξ'' is real.

The incident wave is given by [see Eqs. (1) and (10)]

$$\begin{aligned}
W &= A\cos\gamma(x+ct) \\
\psi_x &= -AM'\gamma^{-1}\sin\gamma(x+ct) \qquad\qquad (23) \\
\psi_y &= 0
\end{aligned}$$

The slow reflected wave [Eq. (11)] becomes

$$w' = A\cos\gamma(x-ct+\ell_1)$$
$$\psi_x' = -AM\gamma^{-1}\sin\gamma(x-ct+\ell_1)$$
$$\psi_y' = 0$$

and the fast reflected wave [Eq. (12)] is given by

$$w'' = (a_2^2+b_2^2)^{1/2} e^{-\gamma'' x} \cos(\gamma ct-\ell_2)$$
$$\psi_x'' = (\gamma'')^{-1}(5\delta_0^4-\gamma''^2)w''$$
$$\psi_y'' = 0$$

In the above,

$$\ell_k = \arctan\frac{b_k}{a_k}\ , \quad k=1,2$$

We see that the slow reflected wave has the same amplitude, wave-length and velocity as the incident wave, but is out of phase with it. The fast reflected "wave" is, in fact, a vibration, the amplitude of which decreases exponentially as the distance from the edge of the plate increases. As $A''' = 0$ by Eq. (22), no other waves are reflected.

Now consider

$$\underline{\gamma^2 RS > R+S}$$

Equations (22) are then replaced by

$$\frac{A'}{A} = \frac{\gamma''(5\delta_0^4-\gamma''^2)+\gamma(5\delta_0^4-\gamma^2)}{\gamma''(5\delta_0^4-\gamma''^2)-\gamma(5\delta_0^4-\gamma^2)}$$

$$\frac{A''}{A} = \frac{2(5\delta_0^4-\gamma^2)\gamma''}{\gamma(5\delta_0^4-\gamma^2)-\gamma''(5\delta_0^4-\gamma''^2)}$$

$$\frac{A'''}{A} = 0$$

The incident wave remains unchanged [Equations (23)], the slow reflected wave becomes

$$
\begin{aligned}
w' &= A' \cos f (x - ct) \\
\psi_x' &= -A' M' f'^{-1} \sin f (x - ct) \\
\psi_y' &= 0,
\end{aligned}
\qquad (26)
$$

the fast reflected wave is given by

$$
\begin{aligned}
w' &= A'' \cos f'' (x - c''t) \\
\psi_x' &= -A'' M'' (f'')^{-1} \sin f'' (x - c''t) \\
\psi_y'' &= 0,
\end{aligned}
\qquad (27)
$$

and the reflected shear wave again vanishes. (The amplitude ratios A'/A and A''/A for this case are plotted versus hf in Fig. 4.)

The incident wave is seen to give rise to two reflected flexural waves; we may examine the manner in which the energy per unit length of wave-front, per cycle, of the incident wave is distributed to the two reflected waves. Using the expressions for energy given in Reference [4], we find

$$
\frac{E'}{E} = \left(\frac{A'}{A}\right)^2
$$

$$
\frac{E''}{E} = \left(\frac{A''}{A}\right)^2 \left(\frac{f}{f''}\right) \frac{\bar{\delta}_c^4 + M''^2}{\bar{\delta}_0^4 + M'^2} .
$$

Here E, E' and E'' are, respectively, the energy per cycle, per unit length of wave front of the incident wave, for the incident, slow reflected and fast reflected waves. The ratios E'/E and E''/E are plotted versus hf in Fig. 5.

The motion corresponding to

$$\gamma^2 RS = R+S$$

may be found by proceeding to the limit, as $\gamma^2 RS \to R+S$, in either of the preceding cases. By either method it may be verified that an incident wave

$$\begin{aligned} w &= A\cos\gamma(x+ct) \\ \psi_x &= A\sqrt{\frac{R}{S(R+S)}}\sin\gamma(x+ct) \\ \psi_y &= 0 \end{aligned} \tag{28}$$

now gives rise to a slow reflected wave,

$$\begin{aligned} w' &= -A\cos\gamma(x-ct) \\ \psi_x' &= -A\sqrt{\frac{R}{S(R+S)}}\sin\gamma(x-ct) \\ \psi_y' &= 0 \end{aligned} \tag{29}$$

and to a <u>thickness-shear vibration</u>,

$$\begin{aligned} w'' &= 0 \\ \psi_x'' &= 2A\sqrt{\frac{S}{R(R+S)}}\sin\gamma ct \\ \psi_y'' &= 0 \end{aligned} \tag{30}$$

The circular frequency p for this vibration is [see Eqs. (3), (5), (6), (8), (9)]

$$p = \kappa c_s \frac{\sqrt{12}}{h}$$

Now, the circular frequency, $\bar{p}$, of the first antisymmetric mode of thickness-shear vibration of an infinite plate, according to the three-dimensional theory

of elasticity, is

$$\bar{p} = \frac{\pi c_s}{h}$$

Thus it seems appropriate to let

$$\kappa = \frac{\pi}{\sqrt{12}}$$

so that the thickness-shear vibration in the present case will occur at the frequency predicted by exact theory for an infinite plate of the same thickness.

It is interesting to notice that the motion here being considered, is one of the possible modes of motion of an infinite strip of thickness h and width b (see Reference [3]), provided

$$b = \frac{hn\pi}{[3(R/S+1)]^{1/2}}, \quad n = 1, 2, \ldots$$

Hence, for $\gamma^2 RS = R + S$, i.e., for $p = \bar{p}$, the semi-infinite plate may be regarded as consisting of an infinite number of independently vibrating strips, each with its infinite dimension parallel to the edge of the plate.

To conclude the discussion of normal incidence, we consider two limiting cases:

When the wave-length of the incident wave is large in comparison with the thickness of the plate, we find, by proceeding to the limit in Equations (22)-(25), as $h\gamma \to 0$,

$$w = A\cos\gamma(x+ct)$$
$$\psi_x = A\gamma\sin\gamma(x+ct)$$
$$\psi_y = 0$$

$$w' = -A\sin\gamma(x-ct)$$
$$\psi_x' = -A\gamma\cos\gamma(x-ct)$$
$$\psi_y' = 0$$

$$w'' = Ae^{-\gamma x}(\cos\gamma ct + \sin\gamma ct)$$
$$\psi_x'' = -A\gamma e^{-\gamma x}(\cos\gamma ct + \sin\gamma ct)$$
$$\psi_y'' = 0$$

$$w''' = 0$$
$$\psi_x''' = 0$$
$$\psi_y''' = 0$$

These expressions show that the incident wave is reflected without change in amplitude or phase velocity, and that a vibration, confined primarily to a region near the edge of the plate, takes place. The classical theory of plates (whose range of applicability is restricted to the limiting case under consideration) predicts the same results.

For wave-lengths which are very small in comparison with the plate thickness[3], we let $h\gamma$ approach infinity in Equations (26), (27) with the result

$$w = A\cos\gamma(x+ct), \quad \psi_x = \psi_y = 0$$
$$w' = A\cos\gamma(x-ct), \quad \psi_x' = \psi_y' = 0$$
$$w'' = \psi_x'' = \psi_y'' = 0$$
$$w''' = \psi_x''' = \psi_y''' = 0$$

3. The theory is not expected to be good for very short waves. This limiting case is included for the sake of completeness.

The total motion is

$$w^* = 2A \cos \gamma x \cos \gamma c t$$

which is a standing wave.

7. Oblique Incidence

We have seen that fundamentally different states of motion obtain according as the circular frequency of the incident wave is less than, equal to, or greater than the circular frequency of thickness-shear vibration of an infinite plate. Hence, for $0 < \alpha < \pi/2$ we shall again examine separately the cases $p<\bar{p}$, $p>\bar{p}$ and $p=\bar{p}$.

$\underline{p<\bar{p}}$

As $p<\bar{p}$ is equivalent to $RS\delta_0^4 < 1$, we see from Equations (20) and (21) that γ'' and γ''' are imaginary.

Setting

$$\bar{\gamma}'' = -i\gamma'', \bar{\gamma}''' = -i\gamma'''$$

we get, from Equation (17),

$$\sin\alpha^j = -\frac{i\gamma}{\bar{\gamma}^j} \sin\alpha \quad , \quad j = '', '''$$

whence

$$\cos\alpha^j = \left[1 + \left(\frac{\gamma}{\bar{\gamma}^j}\right)^2 \sin^2\alpha\right]^{1/2} = m^j \text{ , say.}$$

(For all values of α and γ we have, as noted earlier, $\gamma' = \gamma$, $c' = c$, $\alpha' = \alpha$.)

Substituting into the general expressions for the various reflected waves [Equations (11), (12), (13)], we get from Equations (1),

$$
\begin{aligned}
w' &= A' \exp[i\gamma(x\cos\alpha + \xi)] \\
\psi'_x &= w' M' \gamma^{-1} \cos\alpha \\
\psi'_y &= w' M'_1 \gamma^{-1} i \sin\alpha
\end{aligned}
$$

$$
\begin{aligned}
w'' &= A'' \exp(i\gamma\xi - \gamma'' m'' x) \\
\psi''_x &= w'' M'' m'' \\
\psi''_y &= -w'' M'' (\gamma'')^{-1} \gamma \sin\alpha
\end{aligned}
\qquad (31)
$$

$$
\begin{aligned}
w''' &= 0 \\
\psi'''_x &= A''' i\gamma \sin\alpha \exp(i\gamma\xi - \gamma''' m''' x) \\
\psi'''_y &= A''' \gamma''' m''' \exp(i\gamma\xi - \gamma''' m''' x)
\end{aligned}
$$

where

$$\xi = y\sin\alpha - ct$$

These expressions are valid for all α with the possible exception of $\alpha = \pi/2$, i.e., "grazing" incidence. For that case, the solution of Equations (18) is

$$\frac{A'}{A} = -1, \quad A'' = A''' = 0$$

and we get, in place of Equations (31),

$$w' = -w, \quad \psi_x' = -\psi_x, \quad \psi_y' = -\psi_y$$
$$w^j = \psi_x^j = \psi_y^j = 0, \quad j = '', '''$$

so that the entire motion is then [see Eq. (14)]

$$w^* = \psi_x^* = \psi_y^* = 0. \tag{32}$$

This complete disappearance of the motion is analogous to the case of grazing incidence in the reflection of plane waves from the plane boundary of a semi-infinite solid. We shall return to this question later on.

The waves described by Equations (31) are

1 - a slow flexural wave, reflected at an angle equal to the angle of incidence of the incident wave,

2 - a fast flexural wave of amplitude decreasing exponentially with departure from the edge, and propagated in a direction parallel to the edge,

3 = a shear wave of exponentially decreasing amplitude, propagated along the edge. (See Fig. 6.)

Turning now to the case

$$\underline{p > \bar{p}}$$

we note that, from Equations (20) and (21)

$$\frac{\gamma''}{\gamma} < 1, \quad \frac{\gamma'''}{\gamma} < 1 \quad \text{and} \quad \frac{\gamma''}{\gamma} < \frac{\gamma'''}{\gamma} \quad \text{for all } \gamma.$$

(Fig. 8 illustrates these facts for $\mu = 1/4$.)

Equation (17) permits us to construct a table which shows the relationship between α and α', α'', α''' in terms of trigonometric functions of these angles.

$\sin\alpha = 0$	$\sin\alpha = 0$	$\sin\alpha' = 0$	$\cos\alpha' = 1$		
$0 < \sin\alpha < \gamma''/\gamma$	$0 < \sin\alpha < \gamma''/\gamma$	$\sin\alpha < \sin\alpha' < 1$	$0 < \cos\alpha' < 1$	$\sin\alpha < \sin\alpha'' < \sin\alpha'$	$0 < \cos\alpha'' < 1$
$\sin\alpha = \gamma''/\gamma$	$\sin\alpha = \gamma''/\gamma$	$\sin\alpha' = 1$	$\cos\alpha' = 0$	$\sin\alpha < \sin\alpha'' = \gamma'/\gamma'' < 1$	$0 < \cos\alpha'' < 1$
$\gamma''/\gamma < \sin\alpha < \gamma'''/\gamma$	$\gamma''/\gamma < \sin\alpha < \gamma'''/\gamma$	$\sin\alpha' > 1$	$\cos\alpha'$ imag.	$\sin\alpha < \sin\alpha'' < 1$	$0 < \cos\alpha'' < 1$
$\sin\alpha = \gamma'''/\gamma$	$\sin\alpha = \gamma'''/\gamma$	$1 < \sin\alpha' = \gamma/\gamma''$	$\cos\alpha'$ imag.	$\sin\alpha'' = 1$	$\cos\alpha'' = 0$
$\gamma'''/\gamma < \sin\alpha < 1$	$\gamma'''/\gamma < \sin\alpha < 1$	$\sin\alpha' > 1$	$\cos\alpha'$ imag.	$1 < \sin\alpha''$	$\cos\alpha''$ imag.
$\sin\alpha = 1$	$\sin\alpha = 1$	$1 < \sin\alpha' = \gamma/\gamma'$	$\cos\alpha'$ imag.	$1 < \sin\alpha'' = \gamma/\gamma''$	$\cos\alpha''$ imag.

With the help of this table and Equations (10)-(13) we can now describe the motion associated with various angles of incidence.

For $0 \leq \sin\alpha < \gamma''/\gamma$, the reflected waves are

1 - a slow flexural wave,

2 - a fast flexural wave,

3 - a shear wave.

These emerge at angles α', α'', α''' with

$$\alpha = \alpha' < \alpha''' < \alpha'' < \pi/2$$

as shown in Fig. 7. For instance, with $h\gamma = 5$, we have $\gamma''/\gamma = .302$, $\gamma'''/\gamma = .593$. Taking $\alpha = 15°$ (so that $\sin\alpha < .302$) we get

$$\alpha' = 15°$$

$$\alpha'' = \text{arc sin} \frac{.259}{.302} = 59.1°$$

$$\alpha''' = \text{arc sin} \frac{.259}{.593} = 25.9°$$

For $\sin\alpha = \frac{\gamma''}{\gamma}$, the amplitude ratios [see Eqs. (18)] are

$$\frac{A'}{A} = 1, \quad \frac{A''}{A} = \frac{2(5\delta_0^4 - \gamma^2)}{\nu(5\delta_0^4 - \gamma''^2)}\left[\left(\frac{\gamma''}{\gamma}\right)^2(1-\nu) - 1\right], \quad \frac{A'''}{A} = 0.$$

Thus we have only two reflected waves, (see Fig. 9),

(1) - a slow flexural wave whose angle of emergence is equal to the angle of incidence of the incident wave,

(2) - a fast flexural wave propagated along the free edge.

With $h\gamma = 5$, as in the numerical example above, the critical angle, α_c, for which the shear wave vanishes, is

$$\alpha_c = \text{arc sin } (.302) = 17.6^\circ$$

Letting α increase further, until $\delta''/\delta < \sin\alpha < \delta'''/\delta$, we find that the fast flexural wave [Equations (12)] changes in character since $\cos\alpha''$ is now imaginary. The shear wave reappears and we have (Fig. 10)

(1) - a slow flexural wave,

(2) - an exponentially decaying fast flexural wave, propagated parallel to the edge,

(3) - a shear wave emerging at an angle, α''', with $\alpha < \alpha''' < \pi/2$.

Another critical value of α is reached when $\sin\alpha = \delta'''/\delta$. We then find (Fig. 11)

(1) - a slow flexural wave,

(2) - an exponentially decaying fast flexural wave,

(3) - a shear wave.

Both (2) and (3) are now propagated along the edge. With $h\gamma = 5$, the critical value for α is 36.4°.

Finally, for $\delta'''/\delta < \sin\alpha < 1$, the shear wave also acquires an exponentially decaying amplitude, giving us (Fig. 12)

(1) - a slow flexural wave,

(2) - an exponentially decaying fast flexural wave,

(3) - an exponentially decaying shear wave.

Grazing incidence, i.e., $\alpha = 90^\circ$, leads to vanishing motion, as it did for $p < \bar{p}$.

To complete the discussion of oblique incidence, we consider the case

$$\underline{p = \bar{p}}$$

As the circular frequency of the incident wave approaches the thickness-shear frequency, the amplitudes of the fast reflected wave and of the reflected shear wave become infinite. The resonance encountered here is due to the fact that reflection at the edge of the plate is equivalent to "forcing" the plate at a frequency equal to a "natural" frequency. For, it may easily be verified that the vibration

$$w = \psi_x = 0$$
$$\psi_y = Be^{ipt}$$

is a motion which satisfies the equations of motion (2) and leaves the edge $x = 0$ free of traction.

8. Grazing Incidence

We have seen [Eq. (32)] that the wave motion in a semi-infinite plate disappears as the angle of incidence approaches 90°. A similar situation obtains in the case of waves reflected from the plane boundary of a semi-infinite solid. By application of a suitable limiting process, wave motions for the latter case have recently been found by Goodier and Bishop [4]. A similar limiting process for the present case will now be considered.

Letting

$$\epsilon = \pi/2 - \alpha$$

and neglecting higher powers of ϵ, we have, from Equations (17),

$$\sin\alpha^j = \frac{f}{f_j}\left(1 - \frac{\epsilon^2}{2}\right), \quad j = 1, 4.$$

Substituting into Equations (18), the amplitude ratios are found to be of the form

$$\frac{A'}{A} = -(1+a'\epsilon), \quad \frac{A''}{A} = a''\epsilon, \quad \frac{A'''}{A} = a'''\epsilon \tag{33}$$

Expanding the exponentials which appear in the expressions for displacements, we get from Equations (10)-(13) and Equation (1),

$$\begin{aligned} W &= A(1-i\gamma\epsilon x)\exp(i\gamma\xi) \\ W' &= A'(1+i\gamma\epsilon x)\exp(i\gamma\xi) \\ W'' &= A''\exp(i\gamma\xi - xf'') \\ H''' &= A'''\exp(i\gamma y - xf''') \end{aligned} \tag{34}$$

where

$$\begin{aligned} \xi &= y - ct \\ f^j &= [\gamma^2 - (\gamma^j)^2]^{1/2}, \quad j = '', '''. \end{aligned}$$

These expansions are valid only when higher powers of $\gamma\epsilon x$ can be neglected, that is, for a range of distances from the edge which is small in comparison with the wave-length of the incident wave.

From Equations (14), (32) and (34), the total motion is characterized by the expressions

$$W^* = A\epsilon[-a' - 2i\gamma x + a''e^{-f''x}]\exp(i\gamma\xi) \tag{35}$$

$$H''' = A\epsilon a'''\exp(i\gamma y - xf''') . \tag{36}$$

If we now permit A to become infinite as ϵ approaches zero, and let the approach to infinity be such that the product $A\epsilon$ remains finite, we see that the first term of Equation (35) represents an incident flexural wave while the second term corresponds to the " P_y " wave found by Goodier and Bishop. The third term and Equation (36) indicate, respectively, a flexural and a shear wave, each propagated along the edge of the plate, and each having an exponentially increasing or decreasing amplitude, according as p is less than or greater than $\bar{p}$; for $p = \bar{p}$ we again have resonance.

Acknowledgment

The author wishes to thank Professor R. D. Mindlin of Columbia University both for suggesting this problem, and for his helpful advice in its solution.

Bibliography

1. R. D. Mindlin, "Influence of Rotatory Inertia and Shear on Flexural Motions of Isotropic, Elastic Plates," Journal of Applied Mechanics, Vol. 18 (1951), pp. 31-38.

2. A. E. H. Love, Theory of Elasticity, (Cambridge University Press, London, 1927), 4th Ed., p. 176.

3. R. D. Mindlin, "Thickness-Shear and Flexural Vibrations of Crystal Plates," Journal of Applied Physics, Vol. 22 (1951), pp. 316-323.

4. J. N. Goodier and R. E. D. Bishop, "A Note on Critical Reflections of Elastic Waves at Free Surfaces," Journal of Applied Physics, Vol. 23 (1952), pp. 124-126.

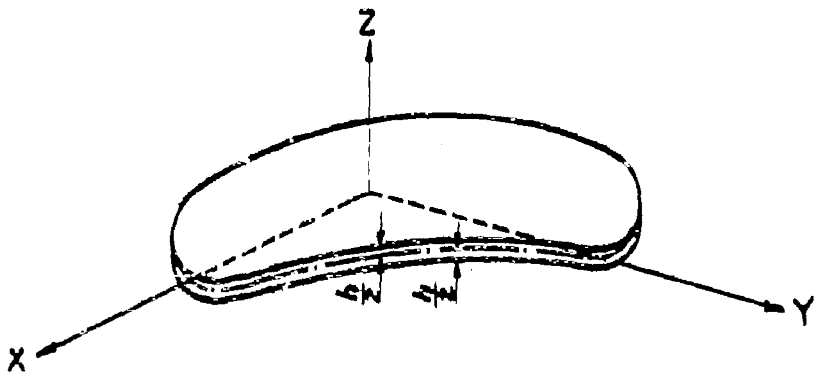

Fig. 1

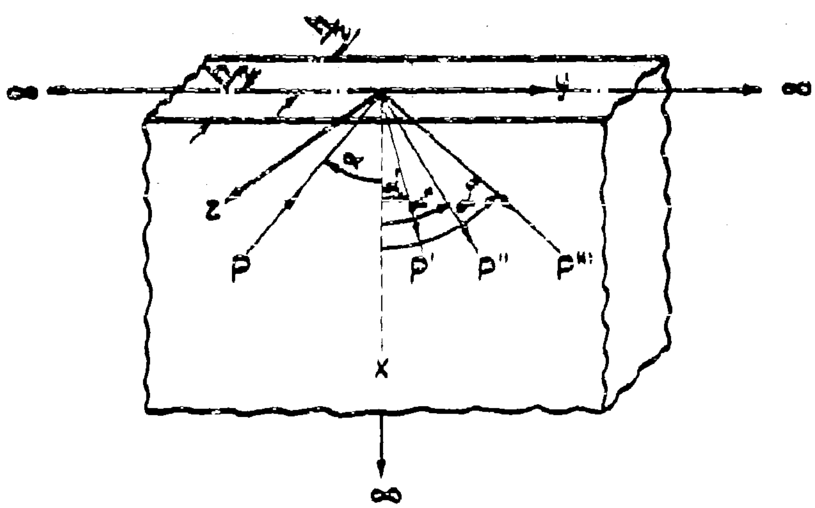

Fig. 2: Incident and Emergent Wave Normals.

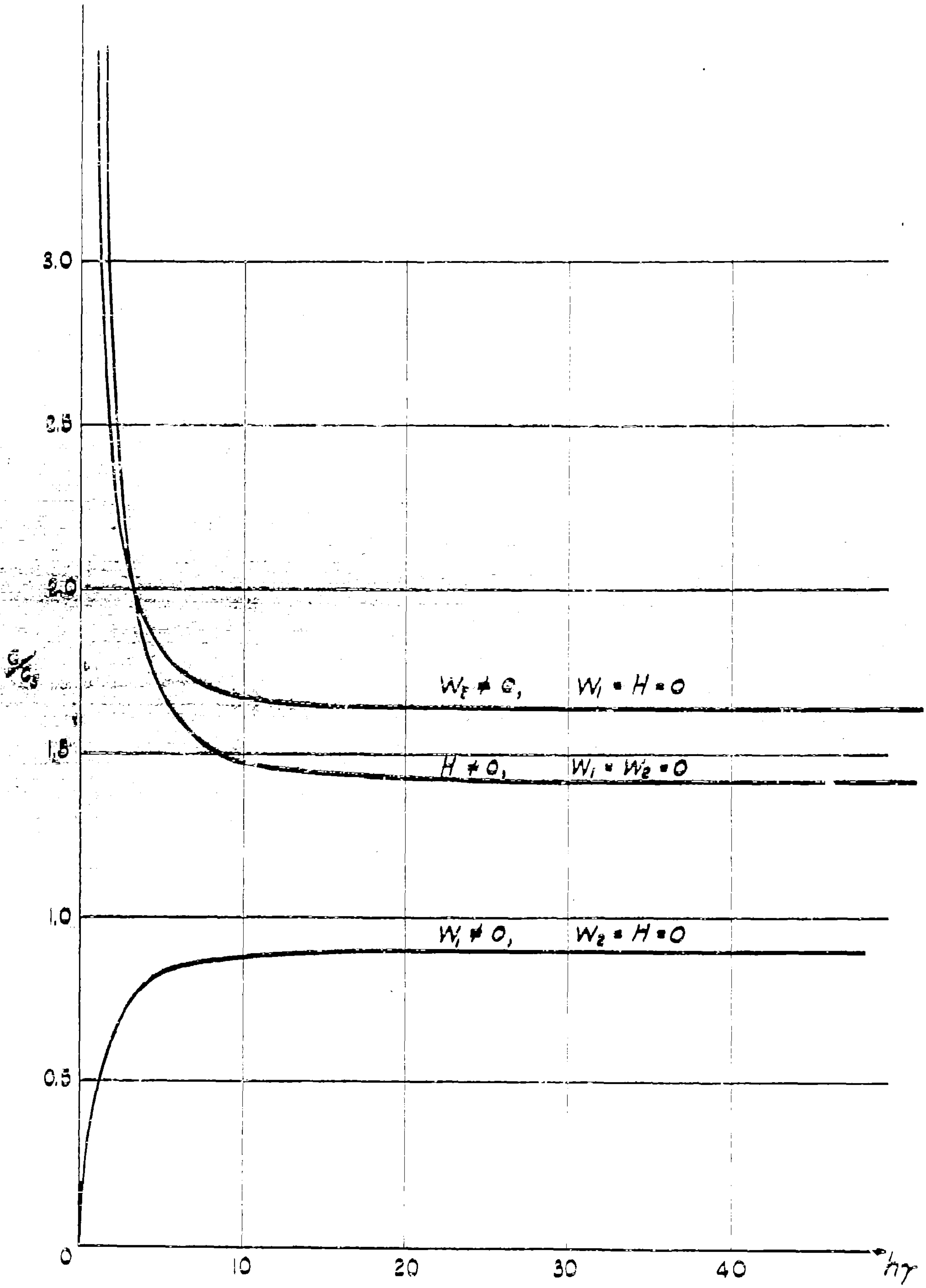

Fig. 3: Relationship between Phase Velocity and Wave Number.

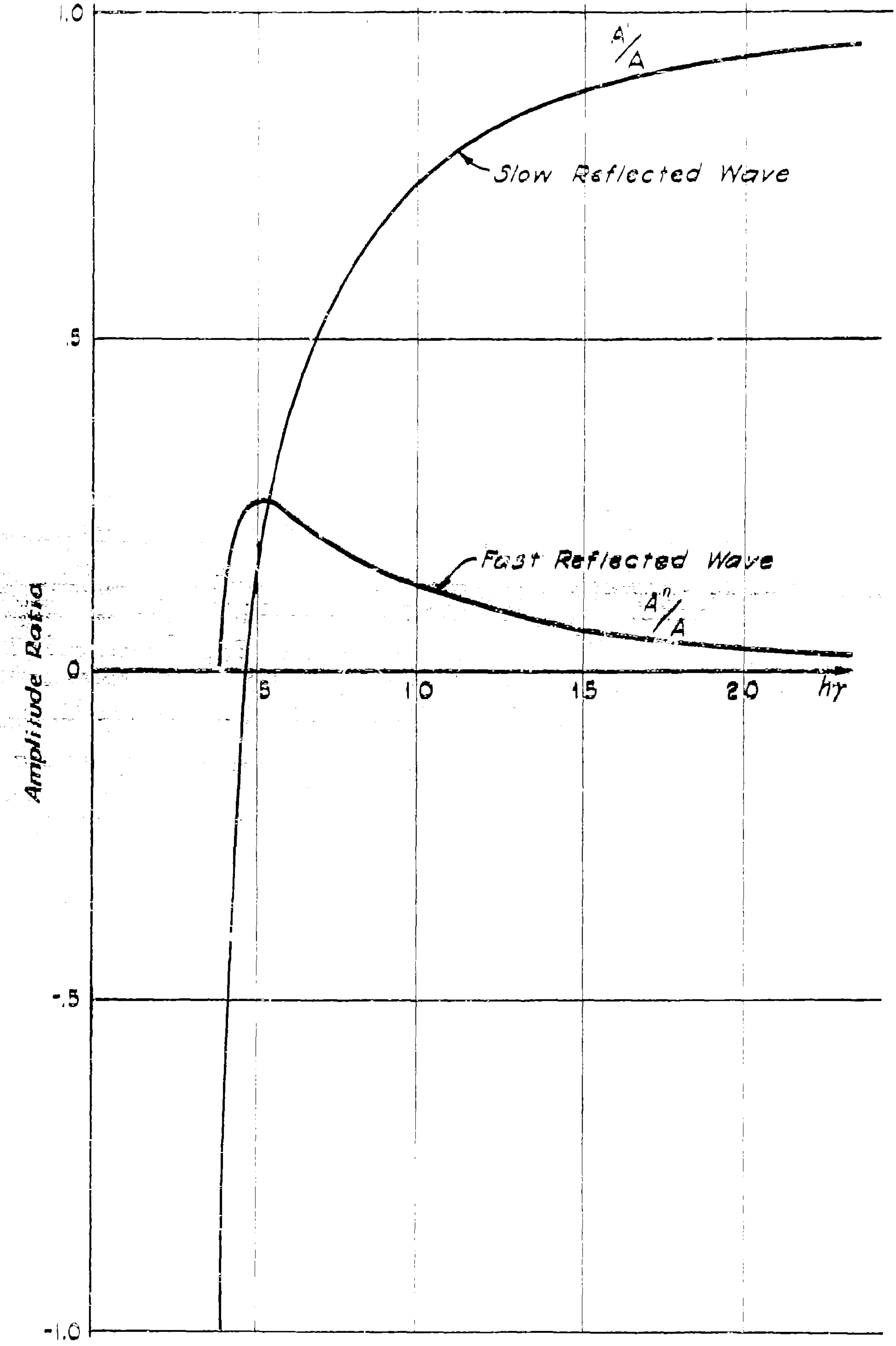

1.0
.5
0
-.5
-1.0
Amplitude Ratio
5
10
15
20
$h\gamma$
A'/A
Slow Reflected Wave
Fast Reflected Wave
A''/A

Fig. 4

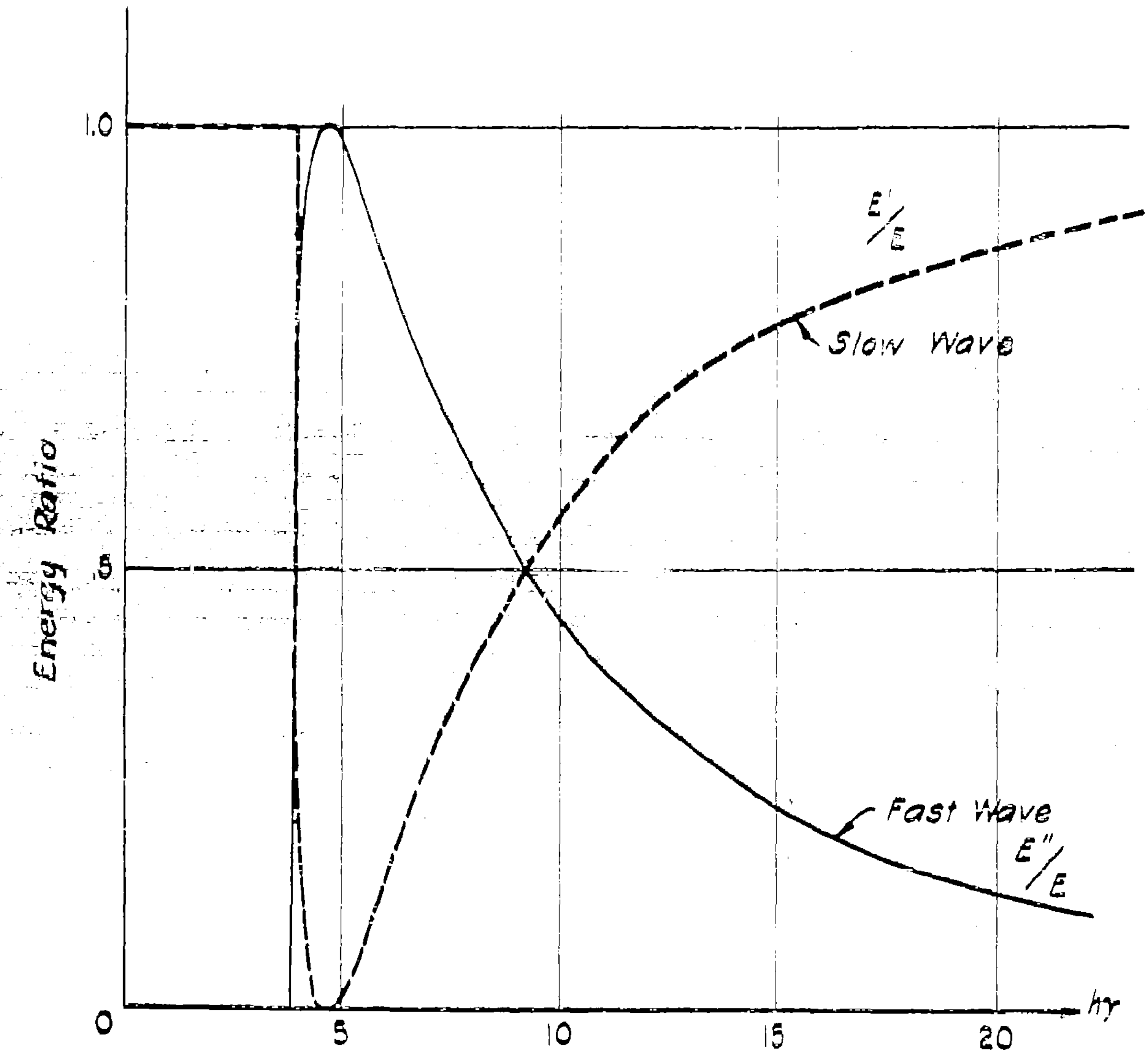

Fig. 5: Energy Partition - Normal Incidence.

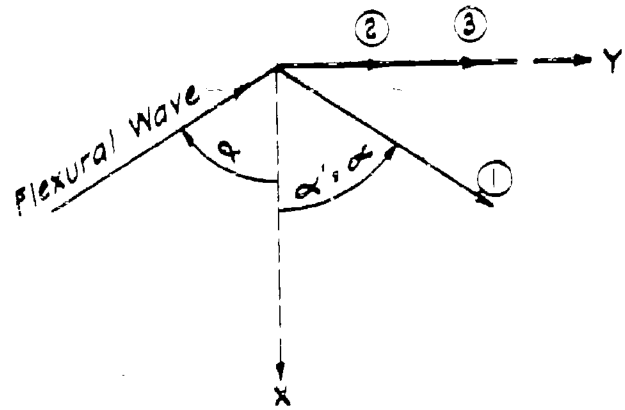

Fig. 6: Oblique Incidence, $p < \bar{p}$.

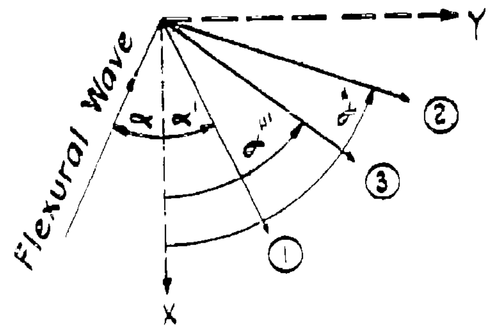

Fig. 7: Oblique Incidence, $p > \bar{p}, 0 \leq \sin\alpha < \bar{r}/r$.

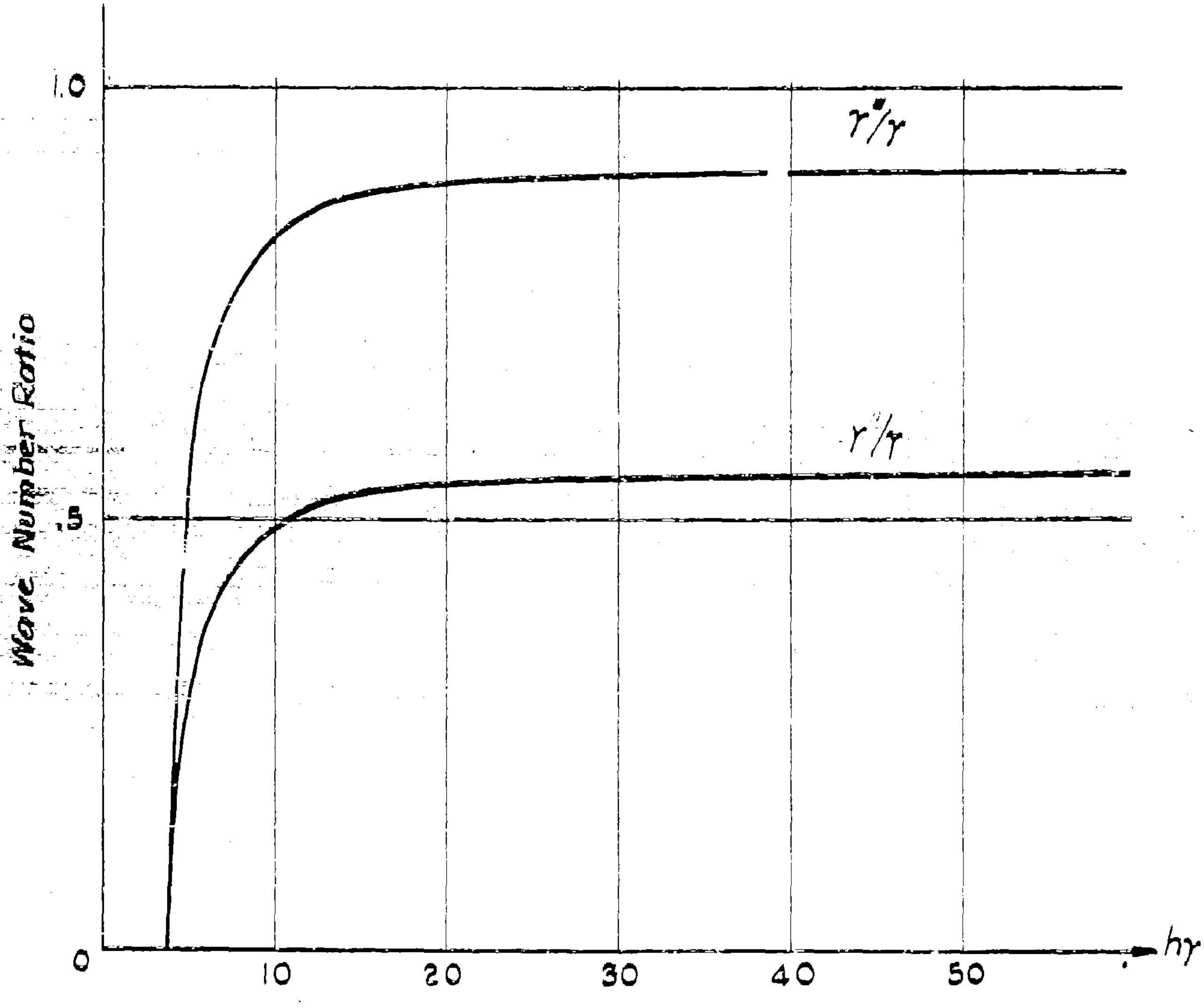

Fig. 8: Wave Number Ratios.

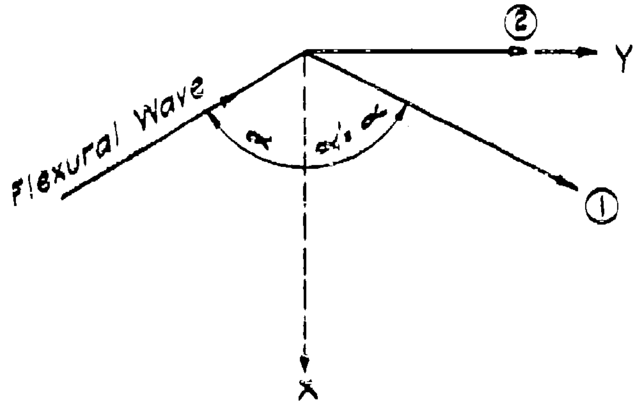

Fig. 9: Oblique Incidence, $p > \bar{p}$, $\sin\alpha = \gamma''/\gamma$.

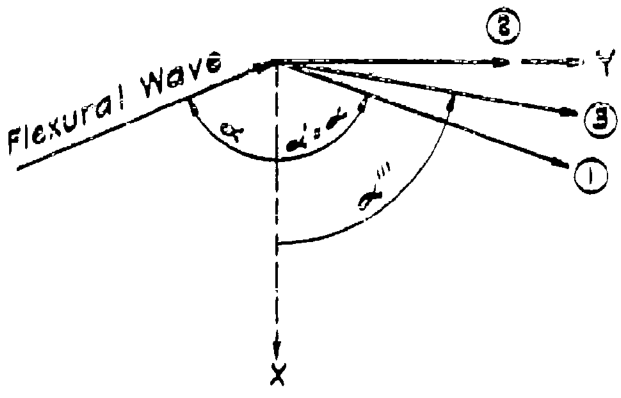

Fig. 10: Oblique Incidence, $p > \bar{p}$, $\gamma''/\gamma < \sin\alpha < \gamma'''/\gamma$.

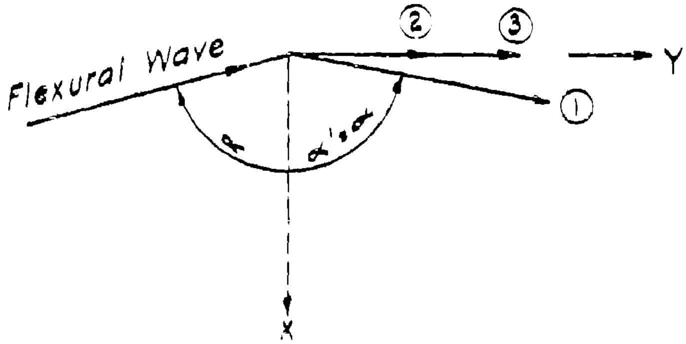

Fig. 11: Oblique Incidence, $p > \bar{p}$, $\sin\alpha = \gamma''/\gamma$.

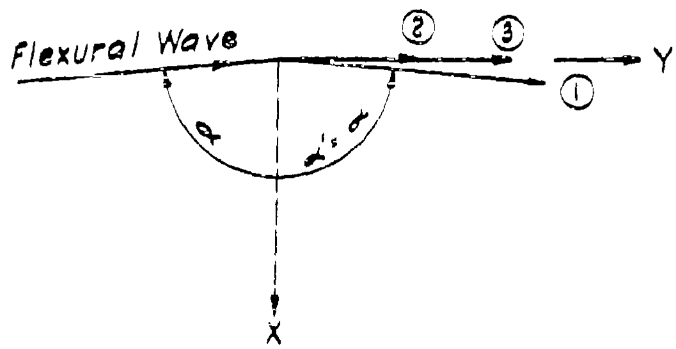

Fig. 12: Oblique Incidence, $p > \bar{p}$, $\gamma''/\gamma < \sin\alpha < 1$.

DISTRIBUTION LIST

for

Technical and Final Reports Issued Under
Office of Naval Research Project NR-064-388, Contract Nonr-266(09)

Administrative, Reference and Liaison Activities of ONR

Chief of Naval Research
Department of the Navy
Washington 25, D.C.
Attn: Code 438 (2)

Director, Naval Research Lab.
Washington 25, D.C.
Attn: Tech. Info. Officer (9)
Technical Library (1)
Mechanics Division (2)
Code 3834 (J. P. Walsh) (1)

Commanding Officer
Office of Naval Research
Branch Office
150 Causeway Street
Boston 10, Massachusetts (1)

Commanding Officer
Office of Naval Research
Branch Office
346 Broadway
New York 13, New York (1)

Commanding Officer
Office of Naval Research
Branch Office
844 N. Rush Street
Chicago 11, Illinois (1)

Commanding Officer
Office of Naval Research
Branch Office
1000 Geary Street
San Francisco 24, California (1)

Commanding Officer
Office of Naval Research
Branch Office
1030 Green Street
Pasadena, California (1)

Contract Administrator, SE Area
Office of Naval Research
c/o George Washington University
707 22nd Street, N.W.
Washington 6, D.C. (1)

Officer in Charge
Office of Naval Research
Branch Office, London
Navy No. 100
FPO, New York, N.Y. (5)

Library of Congress
Washington 25, D.C.
Attn: Navy Research Section (2)

Department of Defense
Other Interested Government Activities

GENERAL

Research and Development Board
Department of Defense
Pentagon Building
Washington 25, D.C.
Attn: Library (Code 3D-1075) (1)

Armed Forces Special Weapons Project
P.O. Box 2610
Washington, D.C.
Attn: Col. G. F. Blunda (1)

GENERAL (cont.)

Joint Task Force 3
12 St. & Const. Ave., N.W. (Temp. U)
Washington 25, D.C.
Attn: Major B. D. Jones (1)

ARMY

Chief of Staff
Department of the Army
Research and Development Division
Washington 25, D.C.
Attn: Chief of Res. and Dev. (1)

ARMY (cont.)

Office of the Chief of Engineers
Assistant Chief for Works
Department of the Army
Bldg. T-7, Gravelly Point
Washington 25, D.C.
Attn: Structural Branch
(R. L. Bloor) (1)

Office of the Chief of Engineers
Asst. Chief for Military Construction
Department of the Army
Bldg. T-7, Gravelly Point
Washington 25, D.C.
Attn: Structures Branch
(H. F. Carey) (1)

Office of the Chief of Engineers
Asst. Chief for Military Operations
Department of the Army
Bldg. T-7, Gravelly Point
Washington 25, D.C.
Attn: Structures Development Branch
(W. F. Woollard) (1)

Engineering Research & Development Lab.
Fort Belvoir, Virginia
Attn: Structures Branch (1)

The Commanding General
Sandia Base, P.O. Box 5100
Albuquerque, New Mexico
Attn: Col. Canterbury (1)

Operations Research Officer
Department of the Army
Ft. Lesley J. McNair
Washington 25, D.C.
Attn: Howard Brackney (1)

Office of Chief of Ordnance
Research & Development Service
Department of the Army
The Pentagon
Washington 25, D.C.
Attn: ORDTB (2)

Commanding Officer
Ballistic Research Laboratory
Aberdeen Proving Ground
Aberdeen, Maryland
Attn: Dr. C. W. Lampson (1)

ARMY (cont.)

Commanding Officer
Watertown Arsenal
Watertown, Massachusetts
Attn: Laboratory Division (1)

Commanding Officer
Frankford Arsenal
Philadelphia, Pennsylvania
Attn: Laboratory Division (1)

Commanding Officer
Squier Signal Laboratory
Fort Monmouth, New Jersey
Attn: Components and Materials
Branch (1)

NAVY

Chief of Bureau of Ships
Navy Department
Washington 25, D.C.
Attn: Director of Research (2)

Director
David Taylor Model Basin
Washington 7, D.C.
Attn: Structural Mechanics Div. (2)

Director
Naval Engr. Experiment Station
Annapolis, Maryland (1)

Director
Materials Laboratory
New York Naval Shipyard
Brooklyn 1, New York (1)

Chief of Bureau of Ordnance
Navy Department
Washington 25, D.C.
Attn: Ad-3, Technical Library (1)

Superintendent
Naval Gun Factory
Washington 25, D.C. (1)

Naval Ordnance Laboratory
White Oak, Maryland
RFD 1, Silver Spring, Maryland
Attn: Mechanics Division (2)

Naval Ordnance Test Station
Inyokern, California
Attn: Scientific Officer (1)

NAVY (cont.)

Naval Ordnance Test Station
Underwater Ordnance Division
Pasadena, California
Attn: Structures Division (1)
Physics Division (1)

Chief of Bureau of Aeronautics
Navy Department
Washington 25, D.C.
Attn: TD-41, Technical Library (1)

Naval Air Experimental Station
Naval Air Materiel Center
Naval Base
Philadelphia 12, Pennsylvania
Attn: Head, Aeronautical Materials Laboratory (1)

Chief of Bureau of Yards & Docks
Navy Department
Washington 25, D.C.
Attn: Code P-314 (1)

Officer in Charge
Naval Civil Engr. Research and Eval. Laboratory
Naval Station
Port Hueneme, California (1)

Superintendent, U.S. Naval Post Graduate School
Annapolis, Maryland (1)

Commander
U.S. Naval Proving Grounds
Dahlgren, Virginia (1)

AIR FORCES

Commanding General
U.S. Air Forces
The Pentagon
Washington 25, D.C.
Attn: Research & Development Division (1)

Commanding General
Air Materiel Command
Wright-Patterson Air Force Base
Dayton, Ohio
Attn: MCREX-B (E. H. Schwartz) (1)

AIR FORCES (cont.)

Office of Air Research
Wright-Patterson Air Force Base
Dayton, Ohio
Attn: Chief, Applied Mechanics Group (1)

OTHER GOVERNMENT AGENCIES

U.S. Atomic Energy Commission
Division of Research
Washington, D.C. (1)

Argonne National Laboratory
P.O. Box 5207
Chicago 80, Illinois (1)

Director
National Bureau of Standards
Washington, D.C.
Attn: Dr. W. H. Ramberg (1)

U.S. Coast Guard
1300 E Street, N.W.
Washington, D.C.
Attn: Chief, Testing & Development Division (1)

Forest Products Laboratory
Madison, Wisconsin
Attn: L. J. Markwardt (1)

National Advisory Committee for Aeronautics
1724 F Street, N.W.
Washington, D.C. (1)

National Advisory Committee for Aeronautics
Langley Field, Virginia
Attn: Dr. E. Lundquist (1)

National Advisory Committee for Aeronautics
Cleveland Municipal Airport
Cleveland, Ohio
Attn: J. H. Collins, Jr. (1)

U.S. Maritime Commission
Technical Bureau
Washington, D.C.
Attn: Mr. V. Russo (1)

Contractors and Other Investigators Actively Engaged in Related Research

Professor J. R. Andersen
Towne School of Engineering
University of Pennsylvania
Philadelphia, Pennsylvania (1)

Professor Lynn Beedle
Fritz Engineering Laboratory
Lehigh University
Bethlehem, Pennsylvania (1)

Professor C. B. Biezeno
Technische Hoogeschool
Niewe Laan 76
Delft, Holland (1)

Professor M. A. Biot
1819 Broadway
New York, New York (1)

Professor R. L. Bisplinghoff
Massachusetts Institute of Technology
Dept. of Aeronautical Engineering
Cambridge 39, Massachusetts (1)

Dr. Hans H. Bleich
Dept. of Civil Engineering
Columbia University
New York 27, New York (1)

Professor J. A. Bogdanoff
Purdue University
Lafayette, Indiana (1)

Professor B. A. Boley
Dept. of Civil Engineering
Columbia University
New York 27, New York (1)

Professor P. W. Bridgeman
Dept. of Physics
Harvard University
Cambridge, Massachusetts (1)

Professor D. M. Burmister
Dept. of Civil Engineering
Columbia University
New York 27, New York (1)

Dr. V. Cadambe
Assistant Director of the National Physical Laboratory of India
New Delhi 12, India (1)

Dr. G. F. Carrier
Graduate Division of Applied Mathematics
Brown University
Providence, Rhode Island (1)

Mrs. Hilda L. Cooper
150 Ravine Avenue
Yonkers, New York (1)

Dr. Antoine E. I. Craya
Neyrpic
Boite, Postale 52
Grenoble, France (1)

Professor J. P. Den Hartog
Massachusetts Institute of Technology
Cambridge 39, Massachusetts (1)

Dr. Herbert Deresiewicz
Dept. of Civil Engineering
Columbia University
632 West 125th Street
New York 27, New York (1)

Dr. C. O. Dohrenwend
Rensselaer Polytechnic Institute
Troy, New York (1)

Professor T. J. Dolan
Dept. of Theoretical and Applied Mechanics
University of Illinois
Urbana, Illinois (1)

Professor Lloyd Donnell
Dept. of Mechanics
Illinois Institute of Technology
Technology Center
Chicago 16, Illinois (1)

Professor D. C. Drucker
Brown University
Providence, Rhode Island (1)

Dr. W. Eckert
Watson Scientific Computing Laboratory
612 West 116th Street
New York 27, New York (1)

Dr. H. Ekstein
Armour Research Foundation
Illinois Institute of Technology
Chicago 16, Illinois (1)

Engineering Library
Columbia University
New York 27, New York (1)

Professor E. L. Eriksen
University of Michigan
Ann Arbor, Michigan (1)

Professor A. C. Eringen
Illinois Institute of Technology
Technology Center
Chicago 16, Illinois (1)

Dr. W. L. Esmeijer
Technische Hoogeschool
Niewe Laan 76
Delft, Holland (1)

Professor A. M. Freudenthal
Dept. of Civil Engineering
Columbia University
New York 27, New York (1)

Professor B. Fried
Washington State College
Pullman, Washington (1)

Professor K. O. Friedrichs
New York University
Washington Square
New York, New York (1)

Professor M. M. Frocht
Illinois Institute of Technology
Technology Center
Chicago 16, Illinois (1)

Professor J. M. Garrelts
Dept. of Civil Engineering
Columbia University
New York 27, New York (1)

Dean J. A. Goff
University of Pennsylvania
Philadelphia, Pennsylvania (1)

Mr. Martin Goland
Midwest Research Institute
4049 Pennsylvania Avenue
Kansas City 2, Missouri (1)

Dr. J. N. Goodier
Dept. of Mechanical Engineering
Stanford University
Stanford, California

Dr. L. E. Goodman
Dept. of Civil Engineering
University of Illinois
Urbana, Illinois (1)

Dr. R. J. Hansen
Massachusetts Institute of Technology
Dept. of Civil & Sanitary Engineering
Cambridge 39, Massachusetts (1)

Professor R. M. Hermes
University of Santa Clara
Santa Clara, California (1)

Professor G. Herrmann
Dept. of Civil Engineering
Columbia University
New York 27, New York (1)

Professor M. Hetényi
Northwestern University
The Technological Institute
Evanston, Illinois (1)

Professor T. J. Higgins
Dept. of Electrical Engineering
University of Wisconsin
Madison 6, Wisconsin (1)

Dr. N. J. Hoff, Head
Dept. of Aeronautical Engineering
& Applied Mechanics
Polytechnic Institute of Brooklyn
99 Livingston Street
Brooklyn 2, New York (1)

Professor M. B. Hogan
University of Utah
Salt Lake City, Utah (1)

Professor D. L. Holl
Iowa State College
Ames, Iowa (1)

Dr. J. H. Hollomon
General Electric Research Labs.
1 River Road
Schenectady, New York (1)

Dr. W. H. Hoppmann
Dept. of Applied Mechanics
John Hopkins University
Baltimore, Maryland (1)

Institut de Mathematiqués
Université
post. fah 55
Skopje, Yugoslavia (1)

Professor L. S. Jacobsen
Dept. of Mechanical Engineering
Stanford University
Stanford, California (1)

Professor Bruce G. Johnston
University of Michigan
Ann Arbor, Michigan (1)

Professor K. Klotter
Stanford University
Stanford, California (1)

Professor W. J. Krefeld
Dept. of Civil Engineering
Columbia University
New York 27, New York (1)

Professor B. J. Lazan
Dept. of Materials Engineering
University of Minnesota
Minneapolis, Minnesota (1)

Dr. E. H. Lee
Division of Applied Mathematics
Brown University
Providence, Rhode Island (1)

Professor George Lee
Rensselaer Polytechnic Institute
Troy, New York (1)

Professor J. M. Lessells
Massachusetts Institute of Technology
Cambridge 39, Massachusetts (1)

Library, Engineering Foundation
29 West 39th Street
New York, New York (1)

Professor Paul Lieber
Dept. of Engineering
Rensselaer Polytechnic Institute
Troy, New York (1)

Dr. Hsu Lo
Purdue University
Lafayette, Indiana (1)

Professor C. T. G. Looney
Dept. of Civil Engineering
Yale University
New Haven, Connecticut (1)

Dr. J. L. Lubkin
Midwest Research Institute
4049 Pennsylvania Avenue
Kansas City 2, Missouri (1)

Professor J. F. Ludloff
School of Aeronautics
New York University
New York 53, New York (1)

Professor J. N. Macduff
Rensselaer Polytechnic Institute
Troy, New York (1)

Professor C. W. MacGregor
University of Pennsylvania
Philadelphia, Pennsylvania (1)

Professor Lawrence E. Malvern
Dept. of Mathematics
Carnegie Institute of Technology
Pittsburgh 13, Pennsylvania (1)

Dr. J. H. Marchant
Brown University
Providence, Rhode Island (1)

Professor J. Marin
Pennsylvania State College
State College, Pennsylvania (1)

Dr. W. P. Mason
Bell Telephone Laboratories
Murray Hill, New Jersey (1)

Professor R. D. Mindlin
Dept. of Civil Engineering
Columbia University
632 West 125th Street
New York 27, New York (15)

Dr. A. Nadai
136 Cherry Valley Road
Pittsburgh 21, Pennsylvania (1)

Professor Paul M. Naghdi
Dept. of Engineering Mechanics
University of Michigan
Ann Arbor, Michigan (1)

Contractors and Other Investigators Actively Engaged in Related Research (cont.)

Professor N. M. Newmark
Dept. of Civil Engineering
University of Illinois
Urbana, Illinois (1)

Professor Jesse Ormondroyd
University of Michigan
Ann Arbor, Michigan (1)

Dr. W. Osgood
Illinois Institute of Technology
Technology Center
Chicago 16, Illinois (1)

Dr. George B. Pegram
Committee on Government Aided Research
313 Low Memorial Library
Columbia University
New York 27, New York (1)

Dr. R. P. Petersen
Director, Applied Physics Division
Sandia Laboratory
Albuquerque, New Mexico (1)

Mr. R. E. Peterson
Westinghouse Research Laboratories
East Pittsburgh, Pennsylvania (1)

Dr. A. Phillips
School of Engineering
Stanford University
Stanford, California (1)

Professor Gerald Pickett
Dept. of Mechanics
University of Wisconsin
Madison 6, Wisconsin (1)

Dr. H. Peritsky
General Electric Research Labs.
Schenectady, New York (1)

Dr. W. Prager
Graduate Division of Applied Mathematics
Brown University
Providence, Rhode Island (1)

RAND Corporation
1500 4th Street
Santa Monica, California
Attn: Dr. D. L. Judd (1)

Dr. S. Raynor
Armour Research Foundation
Illinois Institute of Technology
Chicago 16, Illinois (1)

Professor E. Reissner
Dept. of Mathematics
Massachusetts Institute of Technology
Cambridge 39, Massachusetts (1)

Professor H. Reissner
Polytechnic Institute of Brooklyn
99 Livingston Street
Brooklyn 2, New York (1)

Dr. Kenneth Robinson
National Bureau of Standards
Washington, D.C. (1)

Professor M. A. Sadowsky
Illinois Institute of Technology
Technology Center
Chicago 16, Illinois (1)

Professor M. G. Salvadori
Dept. of Civil Engineering
Columbia University
New York 27, New York (1)

Dr. F. S. Shaw
Polytechnic Institute of Brooklyn
99 Livingston Street
Brooklyn 2, New York (1)

Dr. Daniel T. Sigley
Applied Physics Laboratory
John Hopkins University
8621 Georgia Avenue
Silver Spring, Maryland (1)

Dr. C. B. Smith
Department of Mathematics
Walker Hall
University of Florida
Gainesville, Florida (1)

Professor C. R. Soderberg
Massachusetts Institute of Technology
Cambridge 39, Massachusetts (1)

Professor R. V. Southwell
Imperial College of Science and Technology
South Kensington
London S.W. 7, England (1)

Professor E. Sternberg
Illinois Institute of Technology
Technology Center
Chicago 16, Illinois (1)

Professor J. J. Stoker
New York University
Washington Square
New York, New York (1)

Mr. R. A. Sykes
Bell Telephone Laboratories
Murray Hill, New Jersey (1)

Professor P. S. Symonds
Brown University
Providence, Rhode Island (1)

Professor J. L. Synge
Dublin Institute for Advanced Studies
School of Theoretical Physics
64-65 Merrion Square
Dublin, Ireland (1)

Professor F. K. Teichmann
Dept. of Aeronautical Engineering
New York University
University Heights, Bronx
New York, New York (1)

Professor S. P. Timoshenko
School of Engineering
Stanford University
Stanford, California (1)

Dr. C. A. Truesdell
Graduate Institute for Applied Mathematics
Indiana University
Bloomington, Indiana (1)

Professor Karl S. Van Dyke
Department of Physics
Scott Laboratory
Wesleyan University
Middletown, Connecticut (1)

Dr. I. Vigness
Naval Research Laboratory
Anacostia Station
Washington, D.C. (1)

Dr. Leonardo Villena
Gran Via J. Antonio 6
Madrid, Spain (1)

Professor E. Volterra
Rensselaer Polytechnic Institute
Troy, New York (1)

Mr. A. M. Wahl
Westinghouse Research Laboratories
East Pittsburgh, Pennsylvania (1)

Professor C. T. Wang
Dept. of Aeronautical Engineering
New York University
University Heights, Bronx
New York, New York (1)

Dr. R. L. Wegel
RFD 2
Peekskill, New York (1)

Professor E. E. Weibel
University of Colorado
Boulder, Colorado (1)

Dr. Alexander Weinstein
Institute of Applied Mathematics
University of Maryland
College Park, Maryland (1)

Professor Dana Young
Yale University
New Haven, Connecticut (1)